



## Sediment microbial fuel cell powering a submersible ultrasonic receiver: New approach to remote monitoring

Conrad Donovan<sup>a</sup>, Alim Dewan<sup>a</sup>, Deukhyoun Heo<sup>b</sup>, Zbigniew Lewandowski<sup>c</sup>, Haluk Beyenal<sup>a,\*</sup>

<sup>a</sup>Gene and Linda Voiland School of Chemical Engineering and Bioengineering, Center for Environmental, Sediment and Aquatic Research, Washington State University, Pullman, WA 99163-2710, USA

<sup>b</sup>School of Electrical Engineering and Computer Science, Washington State University, Pullman, WA 99163-2710, USA

<sup>c</sup>Center for Biofilm Engineering, Montana State University, Bozeman, MT, USA

### HIGHLIGHTS

- ▶ We used sediment microbial fuel cells (SMFCs) to power a submersible ultrasonic receiver (SUR).
- ▶ The SMFC was deployed in the Palouse River, Pullman, WA.
- ▶ The SUR is controlled by the power management system (PMS).
- ▶ The SUR is powered continuously.
- ▶ The developed system could make SMFCs a more viable renewable power source.

### ARTICLE INFO

#### Article history:

Received 25 October 2012

Received in revised form

10 December 2012

Accepted 13 December 2012

Available online 24 January 2013

#### Keywords:

Microbial fuel cell  
Power management  
Sensor  
Remote monitoring

### ABSTRACT

The goal of this study was to develop a power management system (PMS) that could power a submersible ultrasonic receiver (SUR) continuously to keep accurate time and listen to ultrasonic signals when there was enough energy for a complete scan. We developed a PMS and modified the hardware and firmware of the SUR to allow it to be controlled by our PMS. Thus, the SUR became optimized for the SMFC and was controlled by the PMS. The SUR switched to idle mode without stopping the RTC when there was not enough energy for a complete scan. The PMS used a 350-F capacitor to store microbial energy. The SMFC was deployed in the Palouse River, Pullman, WA. The integrated PMS was tested and operated the SUR continuously for six weeks. Our integrated PMS and sensor could make SMFCs a more viable renewable power source for continuous environmental monitoring. We found that the SUR could only be powered continuously if its operation was controlled by the PMS. We believe that future applications of more complex sensors could benefit from our novel approach of controlling the sensor using the PMS for uninterrupted operation even when the data are collected intermittently.

© 2013 Elsevier B.V. All rights reserved.

### 1. Introduction

Remote sensors are used to monitor the environment. One of these sensors is the submersible ultrasonic receiver (SUR), which is an underwater sensor system designed for fisheries or wildlife research. The SUR can detect ultrasonic signals and log the movement of fish and other wildlife tagged with ultrasonic transmitters [4,17]. The SUR is a stand-alone device consisting of a battery system, a microprocessor, flash memory, a real-time clock (RTC), a hydrophone, and an ultrasonic receiver. Among all the

components of the SUR, the battery system is the one that limits the duration for which the receiver can be deployed. The batteries used to power the SUR need to be replaced every 5 to 10 months [15]. Battery replacement is costly and time-consuming, especially when one is dealing with a large array of sensors. Therefore, alternative renewable power sources that allow continuous operation of the RTC are needed.

There are many alternative power sources used for unattended sensors, such as seawater batteries [21], wind turbines [2,12], solar panels [1,18,27], piezoelectric energy generators [24,28], and thermoelectric energy harvesters [6,13]. Each of these has its disadvantages, especially for underwater sensors like the SUR. For example, a seawater battery has a limited life that is dependent on the size of the electrode, wind energy cannot be used in deep-water

\* Corresponding author. Tel.: +1 509 335 6607.

E-mail address: [beyenal@wsu.edu](mailto:beyenal@wsu.edu) (H. Beyenal).

applications, and solar panels are limited to daytime applications and require regular maintenance. Sediment microbial fuel cells (SMFCs) can provide continuous low-level power and do not require maintenance or replacement. It has been shown that SMFCs can be used as an alternative renewable power source for wireless sensors [10,11,25,26].

An SMFC consists of two electrodes made of inert conductive materials such as graphite, stainless steel, and carbon cloth [5,19,23]. One of the two electrodes is buried under the sediment and is called the anode. The second electrode is placed in the water where oxygen is present and is called the cathode (Fig. 1). Electricity is generated by the oxidation of sediment organics by the microorganisms naturally present in the sediment. The oxidation of organic chemicals produces electrons that are captured at the anode and transferred through the external circuit to the cathode. Oxygen is typically reduced to form water at the cathode.

The main advantage of using SMFCs is that the power generation is not limited by the fuel supply because the organic materials present in the sediment are renewable. Also, the electrodes of SMFCs are inert materials and, therefore, the duration of power generation is not limited by the materials of construction. Moreover, SMFCs are suitable for most remote areas, including undersea, where using and replacing batteries is difficult. SMFCs do have some limitations, such as nonlinear scaling up [7], low and variable power generation, and low cell potential [25]. Because of the nonlinear scaling up of the electrodes, it is costly to design a large-scale microbial fuel cell for a field application. Therefore, instead of a large microbial fuel cell, an intermittent energy harvesting scheme, which allows the production of high power in short bursts, is preferred. As reported previously [8,9], intermittent energy harvesting uses the cyclic charging and discharging of a capacitor to harvest energy. The capacitors are connected to SMFCs to store and control microbial energy. When the energy stored in the capacitor reaches a predetermined value, the energy is used to activate the power management system (PMS) and operate the sensors. The PMS converts a low potential to a high potential and delivers the power required by the sensors.

In previous studies, SMFCs were used to operate a low-power (11-mW) [10] and a high-power (2.5-W) temperature sensor [11]. Both sensors were used to monitor ambient temperature, and the data were transmitted wirelessly to a receiver. On the receiving end, the time of the temperature measurement was recorded. In this type of system the sensor operation is independent from the PMS. However, in a SUR, the sensor listens to an ultrasonic signal and

records the time and the signal frequency. For the SUR to record the time of the sensing, it is necessary to operate a real-time clock (RTC) continuously. This type of operation needs a different type of PMS, one that can separately provide uninterrupted power to an RTC. In this study we 1) developed a PMS that can power an RTC continuously and power an SUR intermittently to listen to ultrasonic signals, 2) deployed and evaluated the power generation of an SMFC in the field, 3) characterized the power efficiency of the PMS, and 4) tested the capability of the PMS to operate an SUR for remote monitoring using the SMFC in the field.

## 2. Materials and methods

### 2.1. The submersible ultrasonic receiver

The submersible ultrasonic receiver (SUR) is designed to detect and log the presence and telemetry of ultrasonic signals, which include animals tagged with ultrasonic transmitters (Sonotronics, Inc., Tucson, AZ 85713). The SUR has a microprocessor, flash memory, a real-time clock, a hydrophone, an ultrasonic receiver, and an RS-232 serial port. The circuitry is mounted inside a polycarbonate tube. On one side of the tube, there is a serial port connector and transducer. On the other side, there is an on/off switch and a mounting eye bolt. In the original design there is space for two batteries (Lithium Ion, 3.6 V), but for our use, we removed the batteries and connected the PMS and the SMFC. The SUR scans up to 15 different frequencies using its built in-hydrophone, in the range of 30–90 kHz, measuring and recording the intervals between successive pings from individual transmitters. The data collected by the SUR are retrieved manually using an RS-232 serial port when needed.

### 2.2. The sediment microbial fuel cell

#### 2.2.1. Construction and deployment of the sediment microbial fuel cell

The SMFC was deployed in the Palouse River, Pullman, Washington. A schematic diagram of the SMFC is shown in Fig. 1. The anode was made of a graphite plate (GraphiteStore.com). The plate was 60.96 cm × 30.48 cm × 5.08 cm, and the total projected surface area was 0.201 m<sup>2</sup>. For the electrical connection with the graphite plate, we used insulated copper wire that was glued to the graphite using conductive epoxy (CW2400, CircuitWorks). To prevent water–copper wire/conductive epoxy contact, the graphite plate and copper wire joints were covered with silicon rubber.

The cathode was made significantly larger than the anode because previous experience has revealed that the overall power generation is limited by the cathode reaction. The cathode was made of 12 graphite plates stacked together. Each plate was 30.48 cm × 30.48 cm × 1.26 cm. The projected surface area of the cathode was 2.41 m<sup>2</sup>. The electrical connection with the cathode was made using insulated copper wire. The anode was buried 10 cm below the water–sediment interface, and the cathode was placed 15 cm above the water–sediment interface. The cathode was mounted on a tripod made of wood. The electrical cables from the anode and cathode were connected to the PMS and the SUR. For our experimental purpose, the PMS and SUR were placed by the bank of the river. In an actual application the PMS would be placed inside the polycarbonate tube of the SUR and the entire system would be underwater, as shown in Fig. 1.

#### 2.2.2. Characterization of the sediment microbial fuel cell for intermittent energy harvesting

The power generation of the SMFC was characterized using the intermittent energy harvesting method [8]. Intermittent energy

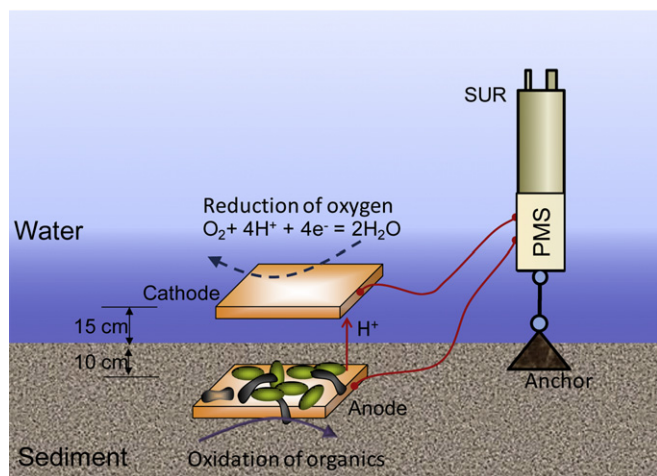


Fig. 1. Schematic diagram of the sediment microbial fuel cell connected to the PMS and the SUR.

harvesting uses the cyclic charging and discharging of a capacitor. Previously, we found that intermittent energy harvesting collects more energy from an SMFC than continuous energy harvesting using a constant load [8]. Since we chose to use a 350-F capacitor for the PMS, we characterized the SMFC for intermittent energy harvesting using a 350-F capacitor. The capacitor was charged and discharged cyclically from a discharging potential ( $V_d$ ) of 0 V to a charging potential ( $V_c$ ) of 500 mV for 112 days (From January to May, 2009). The cyclic charging and discharging was performed automatically using a microbial fuel cell tester as described in our previous publication [9].

The energy stored in the capacitor ( $W_c$ ) when the capacitor was charged from  $V_d$  to  $V_c$  was calculated using Equation (1) [25,26].

$$W_c = \frac{1}{2}C(V_c^2 - V_d^2) \quad (1)$$

The average power ( $P_{avg}$ ) generation in a single charging cycle was calculated by dividing the total energy stored in the capacitor by the charging time, as shown in Equation (2). The charging time ( $t_c - t_d$ ) was calculated by subtracting the time when the capacitor was discharged ( $t_d$ ) from the time when the capacitor was charged ( $t_c$ ).

$$P_{avg} = \frac{W_c}{(t_c - t_d)} = \frac{1}{2} \frac{C(V_c^2 - V_d^2)}{(t_c - t_d)} \quad (2)$$

We used Equation (2) to calculate the power supplied to the SUR. This takes into account the potential change of the capacitor and the duration of operation of the SUR. The  $V_c$  and  $V_d$  values are the capacitor potentials before and after a cycle of scanning by the SUR, respectively. The  $t_c$  and  $t_d$  values are the times before and after the scanning cycle, respectively.

### 2.3. The power management system

The PMS consisted of a capacitor (350 F), startup circuitry, a voltage comparator with an internal voltage reference, two DC/DC converters, and a state machine. Fig. 2 shows a system overview of the main components of the PMS and how it was connected to the SUR and the SMFC. The challenges associated with designing the PMS were 1) the relatively high potential and power requirements compared to what the SMFC could produce, 2) powering the intermittent scanning of the SUR, and 3) powering the RTC continuously. The potential was boosted using the DC/DC converters. The power was generated using the intermittent energy harvesting scheme, which was also controlled by the PMS. During scanning,

the SUR does a frequency scan using its built-in hydrophone and then logs the date, time, and frequency of each detection to the flash memory.

#### 2.3.1. Determining the size of the energy storing capacitor

The size of the capacitor is determined by analyzing the power requirement of the SUR during scanning and the power requirement of the RTC during idle mode. Fig. 3 shows the power flow diagram during the SUR scanning mode (Fig. 3A) and during the SUR idle mode (Fig. 3B). The SUR consumes approximately 15.26 mW in  $20 \pm 2$  s while scanning. In this mode, the power is supplied by DC/DC 2 and DC/DC 1 is turned off. The PMS consumes 21.71 mW to deliver this power, which is generated from the energy stored in the capacitor. The RTC is powered in both scanning and idle modes and requires 1.58 mW at all times. During SUR scanning, power was supplied by DC/DC 2, which is included in the 15.26 mW. While the SUR was in idle mode, power was supplied by DC/DC 1. In this mode, the PMS consumes 1.94 mW, which is generated from the stored energy of the capacitor. Energy from the SMFC is stored in the capacitor, producing between 3 and 10.4 mW on average.

The capacitor size was determined from the maximum power requirement during the scanning. Considering the SUR scanning time, it was calculated that the total energy requirement for each SUR scan cycle was 0.3052 J. To supply this energy to the SUR, DC/DC 2 drew 0.4341 J with an efficiency of 70.3%. This energy was used to calculate the size of the capacitor using Equation (1), with  $V_c$  and  $V_d$  at 517 mV and 514 mV, respectively. The value of  $V_c$  was chosen based on the output potential range of the SMFC. The value of  $V_d$  was chosen based on the tested minimum reliable potential at which DC/DC 2 could begin powering the SUR for scanning without a voltage breakdown due to the large boost ratio and power requirement [20]. From these values, we calculated that a 280.7-F capacitor was needed; since a capacitor of this size was not available, we selected the next available size, 350 F.

#### 2.3.2. The DC/DC converters

The DC/DC converters are used to convert a low potential to a higher potential. The boost ratio, the ratio of the input and output potentials, indicates the magnitude of boosting required. For our SUR system, the required boost ratio ( $V_{out}/V_{in}$ ) for DC/DC 1 was 5.83 and that required for DC/DC 2 was 6.99, assuming the SMFC potential was steady around 515–517 mV. If SMFCs with lower potentials (<515 mV) are used, the PMS and DC/DC converters can be modified to handle the lower potentials. DC/DC 1 was optimized for low current (<1 mA), and DC/DC 2 was optimized for higher current (4–10 mA) requirements.

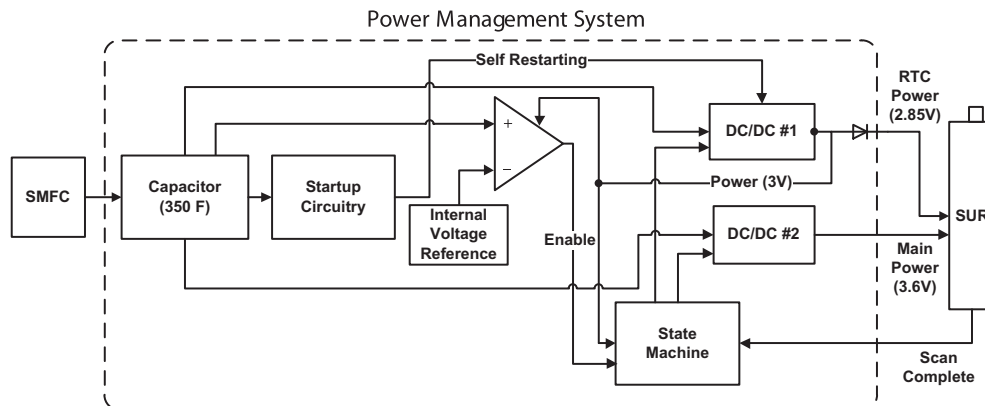
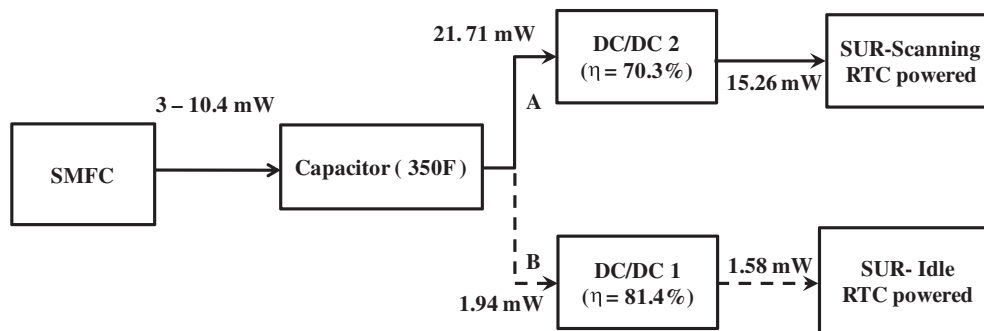


Fig. 2. System overview showing the SMFC, the PMS, and the SUR.



**Fig. 3.** Power flow diagram. A) Power flow for the SUR in scanning mode. In this mode DC/DC 1 is turned off and DC/DC 2 is active. B) Power flow for the SUR in idle mode. In this mode DC/DC 1 is powered on and DC/DC 2 is powered off.

The efficiency of the PMS is determined by measuring the power efficiency of the DC/DC converters, assuming that the power consumption by the other components can be ignored. The bias current of the comparator and the state machine combined was about 30  $\mu$ A, small enough to ignore for our calculations. The startup circuitry, including the charge pump, was only operated for a short time when jump-starting the system was required. The power efficiency ( $\eta$ ) of the DC/DC converter was calculated using the following equation:

$$\eta = \frac{P_{\text{out}}}{P_{\text{in}}} \times 100$$

$P_{\text{out}}$  is the power at the output of the PMS.  $P_{\text{in}}$  is the power at the input of the PMS.

### 2.3.3. State machine

The state machine ensures that the least amount of energy is used during each cycle by immediately removing power from the SUR when the scanning is completed and by using DC/DC 1 and DC/DC 2 only when they are needed. This makes the SMFC more reliable by drawing less power from it. A state diagram of the operation of the PMS is shown in Fig. 4. This state diagram helps illustrate the function of the energy saving mechanism. During the initial state (state 1, Fig. 4), the SUR is idle while power is applied to the RTC to keep accurate time. Once the PMS detects that enough power is available (state 2) for the SUR to begin scanning, the PMS switches states and the SUR begins to scan (state 3). During scanning (state 3), the SUR detects ultrasonic frequencies in the range of 30–90 kHz and writes the detections to nonvolatile flash memory.

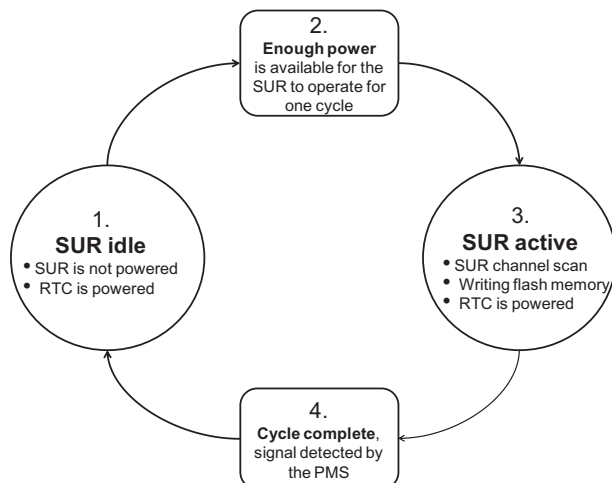


**Fig. 4.** State diagram of the operation of the PMS.

After the SUR finishes scanning, a cycle complete signal is sent to the PMS (state 4) and the SUR is once again in idle mode.

### 2.3.4. System operation

Before connecting the SUR to the PMS, the flash memory of the SUR is erased and the RTC is synchronized to the actual time. Then the PMS and SUR are attached to the SMFC. The state machine receives power from DC/DC 1 at 3 V and monitors the power available in the 350-F capacitor using the comparator. The comparator is also powered by DC/DC 1. The comparator has an internal voltage reference and a wide potential operating range of 1.8 V–5 V. The comparator alerts the state machine when enough power is available for the SUR to start scanning, which enables DC/DC 2. When DC/DC 2 is activated, it provides power at 3.6 V to the SUR for scanning. After the scan is complete, the scan complete line (Fig. 2) is set by the SUR, which is monitored by the state machine. When this signal is received, the state machine shuts down DC/DC 2 and the SUR goes into idle mode. When enough energy is available, the SUR begins to scan once again. While in idle mode, the RTC requires around 2.85 V. This potential is supplied by DC/DC 1. A Schottky diode is required to level shift the 3-V output of the DC/DC 1 to 2.85 V.

A restarting of the system is required in the case of an energy outage by the SMFC. If the power outage is for more than about 2 h, the PMS is automatically switched to sleep mode. When power from the SMFC returns, the PMS is jump-started automatically. Switching the PMS to sleep mode and restarting are done using startup circuitry. The startup circuitry consists of a charge pump and a feedback circuit. If the PMS switches to sleep mode, the times of the detections after restarting are not recorded because the RTC has not been continuously powered. However, the SUR can still scan and log the correct frequency and relative date/time. If the duration of the SMFC power interruption is determined, the date/time of the remaining detections can also be approximated. The startup circuitry includes a charge pump (Seiko Instruments® Inc.) and a feedback circuit. After a restart the PMS operates the same as before.

### 2.3.5. Data logging and collection

SURsoft software (Sonotronics, Inc) was used to upload the data from the flash memory located on the SUR to the computer.

## 2.4. Powering the submersible ultrasonic receiver using the sediment microbial fuel cell in the field

After the SMFC was characterized, the performance of the PMS was tested by continuously powering the SUR for about six weeks. Although the SUR is submersible, for experimental purposes we powered the SUR near the shore. This allowed us to double-check



its operation and monitor the RTC. The anode and the cathode of the SMFC were connected to the negative and positive terminals of the 350-F capacitor. The potentials of the SMFC, the capacitor, the RTC and DC/DC 2 (main power) were monitored using a custom LabView® software application when needed [9].

### 3. Results and discussion

#### 3.1. Characterization of the sediment microbial fuel cell

Fig. 5 shows the anode, cathode, and capacitor potentials of the SMFC during intermittent energy harvesting. The total energy stored in the capacitor in each cycle was 43.75 J, and the average power generation over the period of characterization was  $10.4 \pm 0.3$  mW. This was the maximum average power generation we observed. Because of the variation of environmental conditions, such as water flow and temperature, the power generation of our SMFC varied from 3 to 10.4 mW. Fig. 5 also shows that as the capacitor was charged and discharged the cathode potential varied from  $\sim 35$  to 325 mV (vs. Ag/AgCl) but the anode potential remained unchanged. This variation of the cathode potential indicates that the SMFC power generation was controlled by the performance of the cathode. This shows that to increase power, improvement of the cathode is required.

The average charging time of the capacitor ( $t_c - t_d$ ) was  $1.2 \pm 0.2$  h. This charging time indicates that after the SUR is connected to this SMFC, it will take  $\sim 1.2$  h to start scanning. We should note that once the SMFC starts powering the SUR, the time required for future cycles will not be the same because the potential of the capacitor was designed to drop only about 3 mV during scanning by the SUR. As can be calculated from the charging curves shown in Fig. 5, the charging of the last 3 mV takes an average of 2.5 min, which means that after the first scan the subsequent scans should take less than 2.5 min if the power generation level remains constant. This time will also depend on the variation of environmental variables such as river temperature, water flow, and rain.

#### 3.2. Powering the submersible ultrasonic receiver using the sediment microbial fuel cell

The performance of the SMFC, the SUR, and the PMS was monitored by watching the potential and current variation in the various components. Example data from this operation are

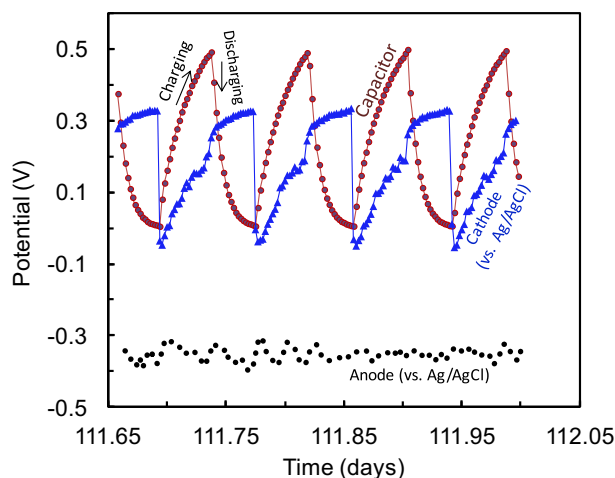


Fig. 5. The anode, cathode, and capacitor potentials of the SMFC during intermittent energy harvesting. The charging potential ( $V_c$ ) was 500 mV, and the discharging potential ( $V_d$ ) was 0 mV.

presented here to describe the performance of the SMFC, the long-term performance of the SUR, and the energy efficiency of the PMS. The output potential of DC/DC 2 was monitored to observe whether the SUR was in scan mode or idle mode. Fig. 6A shows the output potential of DC/DC 2 during the 30-minute window of operation. It shows that during each scan power was drawn by the SUR at a potential of 3.6 V. The duration of the SUR scan was  $\sim 20 \pm 2$  s. The total energy consumption was 0.309 J, which is slightly higher than the designed energy consumption (0.3052 J). The output potential of DC/DC 2 was  $\sim 1$  V when the SUR was in idle mode. After the SUR finished scanning and writing data to the flash memory, a scan complete signal was detected by the state machine, which

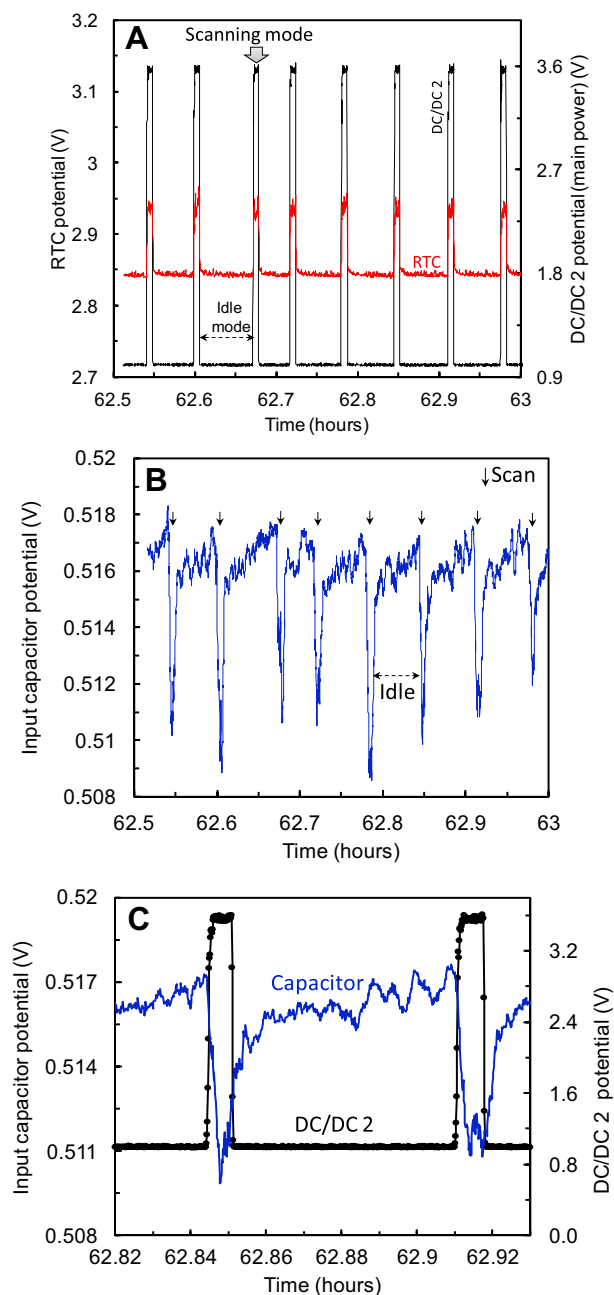


Fig. 6. Variation of DC/DC 2, RTC, and capacitor potentials during field testing of the system using the SMFC. A) DC/DC 2 output potential and the input potential of the real-time clock (RTC). The potential spiked during the scanning. B) Input capacitor potential profile during scanning and in idle mode. The arrow indicates the time when the SUR was scanning. C) Enlargement of the input capacitor and DC/DC 2 output potentials during two scans.

put the SUR into idle mode. When the SUR was in idle mode, power was still supplied to the RTC by DC/DC 1. Fig. 6A also shows the variation of the RTC input potential. While the SUR was in idle mode, the RTC potential was 2.85 V; while it was in scan mode, the bias potential of the RTC increased to 2.95 V.

The potential of the capacitor was the input potential for both DC/DC 1 and DC/DC 2. Fig. 6B shows the input capacitor potential for a window of about 30 min. During this time, the potential changed from ~517 to 510 mV. When the SUR was scanning, the voltage dropped by 7–10 mV. This voltage drop was due to the sudden power demand on the system. Since the SUR operating time was  $20 \pm 2$  s, the potential drop varied, but the average net potential drop was 2.5 mV. Once the SUR was in idle mode, a potential rebound occurred in the capacitor that allowed the potential to return to its equilibrium level of about 515 mV. The rebound potential of the capacitor fluctuated within  $\pm 1$  mV because of power consumption for continuous operation of the RTC. An enlargement of the two scans (Fig. 6C) shows this fluctuation of the input capacitor potential. We should note that part of the variation of capacitor potential may come from a fluctuation of the energy generation by the SMFC. The rebound took  $\sim 3.5$  min, which means that the frequency of SUR scanning was  $\sim 3.5$  min, which is higher than the expected value ( $\sim 3$  min). In the characterization of the SMFC, we found that this potential change of the capacitor would take less than 1 min. The energy accumulation by the capacitor during the potential rebound was 0.3175 J.

### 3.3. Long-term operation of the submersible ultrasonic receiver using the sediment microbial fuel cell

Fig. 7 shows time between the sensor scans during a six-week period. The maximum and minimum scan times were 7.13 min and 1 min, respectively. An average scan time of 2.5 min was observed over the six-week period. The SUR was controlled by software to look at only two frequencies (71 kHz and 72 kHz) when scanning. The fluctuation of the time between scans was determined by the performance of the SMFC. At the end of the six-week period, the SMFC started to lose some power and the time between scans increased. Since the power of an SMFC fluctuates over the course of a year, this change was expected. In our previous study, which was conducted in the same place, we observed a similar power fluctuation due to variation of ambient temperature and changes in water flow caused by rain or snow in the river [10].

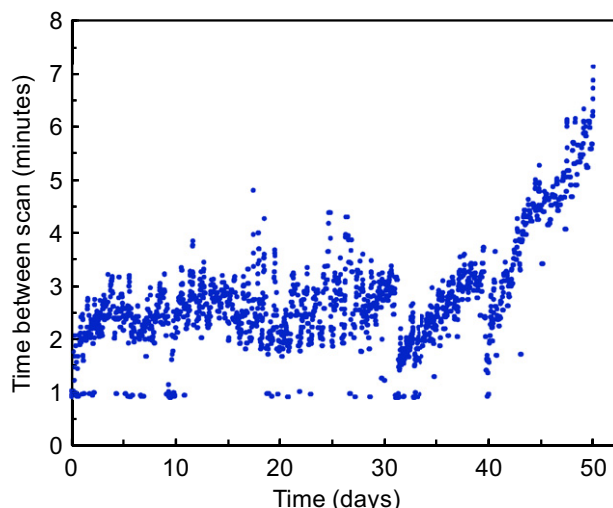


Fig. 7. The time between SUR scans in the long-term field testing.

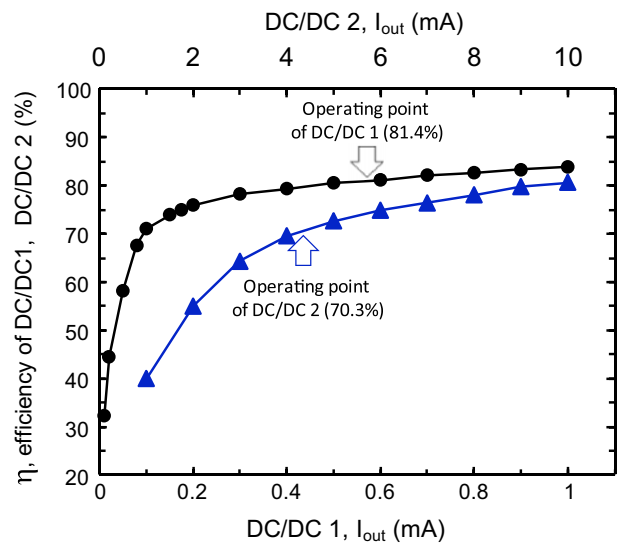


Fig. 8. Measured efficiency of the DC/DC converters when the input potential for both was 500 mV. The DC/DC 1 output was 3 V and the DC/DC 2 output was 3.6 V.

### 3.4. Power efficiency of the power management system

Fig. 8 shows the power efficiency of DC/DC 1 and DC/DC 2 when the input potential was 500 mV for both. The DC/DC 1 output potential was 3 V, while the DC/DC 2 output potential was 3.6 V. To save energy, DC/DC 1 and DC/DC 2 were never operated at the same time. The overall system efficiency varied over time because it depended on the time between scans. Since the PMS only operated one DC/DC converter at a time and other PMS components had negligible power consumption, the efficiency of the system was dominated by the efficiency of whichever DC/DC converter was operating at any given time. When the scanning was less frequent, the efficiency was closer to 81.4%, and when the scanning was more frequent the efficiency decreased to 70.3%. During the six-week period that the data were collected, the total average power efficiency for the power management system was 75.3%.

## 4. Application of the developed power management system to other underwater sensors

The developed SMFCs and PMSs can be used to power other underwater sensors that have power requirements similar to those of the SUR. For example, the acoustic [14,22], piezoelectric [21], thermocouple [11], optical [3], barometric [25], and electrochemical [16] sensors that are used for environmental monitoring, habitat monitoring, seismic monitoring, oceanography, and military surveillance all have power requirements that are in the range from 10 mW to 2.5 W. The main advantage of our PMS is that it can track the time of monitoring using a RTC.

## 5. Conclusions

Our study demonstrated that developed SMFC and PMS can continuously power an underwater hydrophone for long-term battery-less environmental monitoring. Additionally, the SUR hardware and firmware modifications allowed it to be optimized for the PMS, which gave the PMS control of the SUR, saved additional energy and allowed continuous operation of an RTC. We concluded the following:

- A sediment microbial fuel cell producing an average of 3–10.4 mW can power a real-time clock continuously and an

underwater ultrasonic sensor intermittently without the use of batteries.

- A power management system with two DC/DC converters supplying power separately makes the energy harvesting of the sediment microbial fuel cell more efficient and reliable.

## Acknowledgments

The authors gratefully acknowledge grant – #N00014-06-1-0217 – from the U.S. Office of Naval Research (ONR). Conrad Donovan was supported by NSF IGERT (DGE-0900781) and CDADIC. The authors acknowledge Marlin Gregor from Sonotronics, Inc for the hardware and firmware modifications.

## Nomenclature

C	Capacitance (F)
DC/DC	DC to DC converter
DC/DC 1	DC to DC Converter 1
DC/DC 2	DC to DC Converter 2
MFC	Microbial fuel cell
PMS	Power management system
RTC	Real-time clock
SMFC	Sediment microbial fuel cell
SUR	Submersible ultrasonic receiver

## References

- [1] A.A. Alexander, R. Taylor, V. Vairavanathan, Y. Fu, E. Hossain, S. Noghanian, *Wireless Communications & Mobile Computing* 8 (2008) 1255–1276.
- [2] R.J. Ang, Y.K. Tan, S.K. Panda, Energy Harvesting for Autonomous Wind Sensor in Remote Area, in: *IECON 2007: 33rd Annual Conference of the IEEE Industrial Electronics Society*, 1–3 2007, pp. 2104–2109.
- [3] S. Arnon, Swarm of Sensor Acquisition and Identification Using Optical Wireless Communication, in: *Free Space Laser Communications IV*, vol. 5550, 2004, pp. 436–442.
- [4] P.W.S.G.D. Bettoli, D.W. Hubbs, *North American Journal of Fisheries Management* 30 (2010) 989–993.
- [5] D.F. Call, M.D. Merrill, B.E. Logan, *Environmental Science & Technology* 43 (2009) 2179–2183.
- [6] S. Dalola, V. Ferrari, M. Guizzetti, D. Marioli, E. Sardini, M. Serpelloni, A. Taroni, Autonomous Sensor System with RF Link and Thermoelectric Generator for Power Harvesting, in: *2008 IEEE Instrumentation and Measurement Technology Conference*, 1–5 2008, pp. 1376–1380.
- [7] A. Dewan, H. Beyenal, Z. Lewandowski, *Environmental Science & Technology* 42 (2008) 7643–7648.
- [8] A. Dewan, H. Beyenal, Z. Lewandowski, *Environmental Science & Technology* 43 (2009) 4600–4605.
- [9] A. Dewan, C. Donovan, D. Heo, H. Beyenal, *Journal of Power Sources* 195 (2010) 90–96.
- [10] C. Donovan, A. Dewan, D. Heo, H. Beyenal, *Environmental Science & Technology* 42 (2008) 8591–8596.
- [11] C. Donovan, A. Dewan, H.A. Peng, D. Heo, H. Beyenal, *Journal of Power Sources* 196 (2011) 1171–1177.
- [12] C.C. Federspiel, J. Chen, Air-powered Sensor, in: *Proceedings of the IEEE Sensors* 2003, 1–2 2003, pp. 22–25.
- [13] M. Ferrari, V. Ferrari, M. Guizzetti, D. Marioli, A. Taroni, Characterization of Thermoelectric Modules for Powering Autonomous Sensors, in: *2007 IEEE Instrumentation & Measurement Technology Conference*, 1–5 2007, pp. 1708–1713.
- [14] J. Heidemann, W. Ye, J. Wills, A. Syed, Y.A. Li, Research Challenges and Applications for Underwater Sensor Networking, in: *2006 IEEE Wireless Communications and Networking Conference*, 1–4 2006, pp. 228–235.
- [15] <http://sonotronics.com/wp-content/uploads/2010/07/SUR-3.pdf>, 2011. Sonotronics, Inc., Tucson, Arizona, US (accessed 28.03.12).
- [16] T. Ishimaru, H. Ootobe, T. Saino, H. Hasumoto, T. Nakai, *Journal of Oceanographical Society of Japan* 40 (1984) 207–212.
- [17] A.P. Karam, B.R. Kesner, P.C. Marsh, *Journal of Fish Biology* 73 (2008) 719–727.
- [18] R. Lajara, J. Alberola, J. Pelegri-Sebastia, *Sensors* 11 (2011) 329–340.
- [19] B.E. Logan, B. Hamelers, R.A. Rozendal, U. Schröder, J. Keller, S. Freguia, P. Aelterman, W. Verstraete, K. Rabaey, *Environmental Science & Technology* 40 (2006) 5181–5192.
- [20] H. Mahmood, K. Natarajan, Parasitics and Voltage Collapse of the DC-DC Boost Converter, in: *2008 Canadian Conference on Electrical and Computer Engineering*, 1–4 2008, pp. 261–266.
- [21] R. Mijarez, P. Gaydecki, M. Burdekin, *Smart Materials & Structures* 16 (2007) 1857–1869.
- [22] A.K. Othman, A.E. Adams, C.C. Tsimenidis, B. Sharif, Underwater Acoustic Networks Discovery Protocol and Localization, in: *Oceans 2006-Asia Pacific*, 1–2 2006, pp. 1–6.
- [23] P.A. Selemba, M.D. Merrill, B.E. Logan, *Journal of Power Sources* 190 (2009) 271–278.
- [24] Y.K. Tan, S.K. Panda, A Novel Piezoelectric Based Wind Energy Harvester for Low-Power Autonomous Wind Speed Sensor, in: *IECON 2007: 33rd Annual Conference of the IEEE Industrial Electronics Society*, 1–3 2007, pp. 2175–2180.
- [25] L.M. Tender, S.A. Gray, E. Groveman, D.A. Lowy, P. Kauffman, J. Melhado, R.C. Tyce, D. Flynn, R. Petrecca, J. Dobarro, *Journal of Power Sources* 179 (2008) 571–575.
- [26] F. Zhang, L. Tian, Z. He, *Journal of Power Sources* 196 (2011) 9568–9573.
- [27] H.X. Zhang, M. Fallahi, S. Pau, R.A. Norwood, N. Peyghambarian, *Proceedings of SPIE* 7666 (2010) 766621–766626.
- [28] W.L. Zhou, W.H. Liao, W.J. Li, *Proceedings of SPIE* 5763 (2005) 233–240.